An Open-Source and Low-Cost Dual Extruder 3D Printer for Macroscale Biotic Materials

Jesse P. de Alva[a,b], Markus J. Buehler[a,b,c,*]

[a] Laboratory for Atomistic and Molecular Mechanics (LAMM), Massachusetts Institute of Technology, 77 Massachusetts Ave., Cambridge, MA 02139, USA.
[b] Department of Mechanical Engineering, Massachusetts Institute of Technology, 77 Massachusetts Ave., Cambridge, MA 02139, USA
[c] Center for Computational Science and Engineering, Schwarzman College of Computing, Massachusetts Institute of Technology, 77 Massachusetts Ave., Cambridge, MA 02139, USA

*E-mail: mbuehler@mit.edu

Abstract: This work presents the design and fabrication of a novel, dual-extruder biotic 3D printer tailored for precise deposition of natural biomaterials such as pectin, chitosan, and cellulose. Moving beyond the limitations of traditional thermoplastic extrusion which relies on non-renewable plastics and produces significant waste, this printer utilizes a syringe-based mechanical extruder to deposit viscous biotic material hydrogels. The integration of a dual-extruder system enables the creation of multimaterial prints, offering new possibilities for sustainable and biotic manufacturing. Designed with accessibility and versatility in mind, the system features user-friendly operation suitable for non-experts with open-source hardware and software. By providing a robust, customizable, and open-source platform, this work aims to empower researchers, educators, and innovators to advance biomaterials research and expand the reach of sustainable additive manufacturing. The printer fosters a collaborative community and lays the groundwork for further exploration of biological designs and materials.

Keywords: biological materials, biotic materials, sustainability, multimaterial printing

1 Introduction

Modern manufacturing stands at a crossroads, where advancements in materials science drive innovation, yet the environmental toll of synthetic, non-degradable materials, ranging from solid waste accumulation[1] to greenhouse gas emissions[2], poses escalating risks to ecosystems worldwide[3]. In response, biotic materials, derived from renewable and organic sources such as cellulose, chitosan, and pectin, offer a promising class of sustainable alternatives[4–7]. These materials are biodegradable[7,8], exhibit remarkable versatility[9,10], and can often be sourced with minimal environmental impact[11,12]. These materials show early promise across multiple applications such as single use packaging[13], prototyping material[14], or even structural applications[15,16]. However, unlike conventional materials, biotic materials do not yet have a standardized or widely adopted fabrication method. Therefore, realizing the potential of these materials requires new fabrication platforms capable of handling their unique properties while enabling precise control over structure and composition[17,18]. Thus, additive manufacturing is adopted to address these needs[9,16].

In prior work, early biotic 3D printers demonstrated the feasibility of printing with hydrogel-based biotic materials[19]. Unlike traditional Fused Filament Fabrication (FFF), otherwise known as Fused Deposition Modeling (FDM), 3D printers, which melt thermoplastics for layer-by-layer deposition, the biotic printer uses a syringe-based extrusion system to deposit viscous hydrogels. This biomaterial is not melted and resolidified as the print cools but instead relies on drying out its

moisture over time to achieve its final properties. The original proof-of-concept biotic 3D printer primarily served as a tool for raising awareness about biotic materials, often through the creation of large-scale art installations[20]. These machines also demonstrated the feasibility of creating biomaterial gradients using single-extruder 3D printers[21]. While these systems effectively showcased the potential of biotic materials, they were not optimized for high precision, adaptability, or versatile applications, with their exploration constrained by the inherent limitations of single-extruder technology. A major drawback of earlier designs was their reliance on a pneumatic extruder for biomaterial deposition [21]. This system operates by applying user-specified pressure to control the force and volumetric flow rate of the biomaterial. However, pneumatic extruders are highly sensitive to variations in biomaterial viscosity, which could be influenced by factors such as feedstock temperature, ambient humidity, and material age. These inconsistencies often occurred within the same batch of material or even during a single printing session, resulting in unreliable extrusion and flow rates. Additionally, as the cartridge emptied, the extrusion rate would increase, further complicating the process. Due to these challenges, consistent and successful printing demanded significant user expertise. Operators frequently needed to adjust extrusion pressure mid-print, restart the process, and rely on trial and error to achieve an acceptable flow rate. This manual intervention introduced substantial variability into the definition of what constitutes a "good print," undermining the repeatability and reliability of the pneumatic extruder system.

Unlike these early systems, the BEAVER platform introduces a motor-driven, mechanical syringe extrusion mechanism based on a worm-gear and leadscrew design, enabling precise and consistent deposition of viscous hydrogels. Moreover, BEAVER is the first open-source printer to implement dual independently actuated extruders tailored for biotic materials, allowing multi-material printing and compositional gradients. This represents a significant advancement over prior pneumatic and single-material systems, addressing key limitations such as inconsistent flow, lack of modularity, and limited accessibility for non-experts.

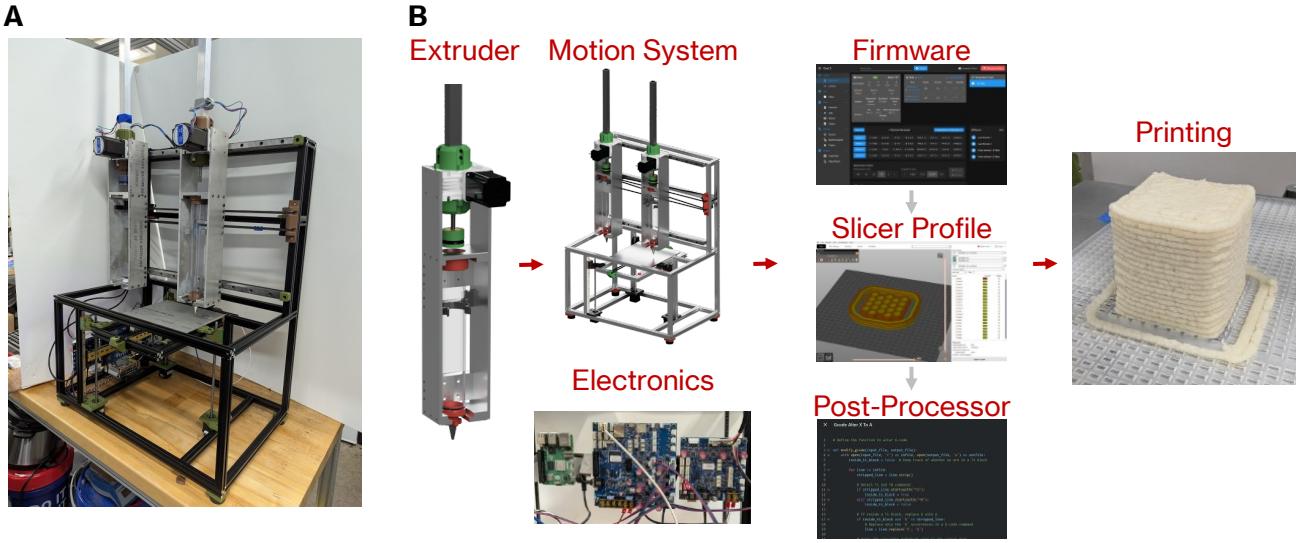

Figure 1: BEAVER Overview. A) Photograph of the assembled BEAVER with dual extruders. B) Process plan of BEAVER. The development begins with the extruder, followed by the parallel development of the motion system and electronics. From there, the firmware configuration is developed, followed by the creation of a printer profile in a designated slicing software and creation of a custom post-processing script before final printing and testing can be achieved.

This work introduces the Biotic Extruder for Additive Volumetric Engineering and Research (BEAVER), a dual-extruder biotic 3D printer designed to process biocomposites with precision and consistency. Here, precision refers to the fine spatial control of deposition paths and feature dimensions, while consistency describes the system's ability to maintain stable extrusion rates and print quality. Developing the printer posed unique engineering challenges, driven by the distinct properties of biotic materials. Unlike thermoplastics in traditional FFF 3D printing, biotic materials are deposited as viscous fluids or gels, remaining malleable during printing, which necessitated entirely new hardware solutions to maintain the feedstock's viscous state. Additionally, the organic nature of biotic materials introduced challenges related to cleanliness and hygiene. These materials are susceptible to mold and degradation if not properly dried and cured, requiring all material-contacting components to be easily cleanable, as inaccessible areas increase contamination risks and potentially compromise material integrity.

Notably, multi-material printing is a critical capability of BEAVER, enabling the creation of advanced biocomposites such as those with compositional gradients and dual-material interactions. Here, compositional gradients refer to controlled transitions in material composition within a single printed part. Multi-material interactions describe spatially programmed combinations of biomaterials. This feature significantly broadens the printer's potential, allowing researchers to explore complex material properties and unlock novel applications in biotic fabrication. Usability is another core focus of the redesign. Designed for researchers without extensive 3D printing expertise, the printer prioritizes intuitive hardware and software workflows. To support the rapidly evolving field of biotic materials research, BEAVER incorporates a forward-thinking, modular design. The system is adaptable to new biocomposites, tools, and techniques, featuring hardware designed for easy upgrades and software capable of managing diverse workflows and material properties. This ensures versatility for both current and future biotic fabrication applications. By addressing these challenges, BEAVER contributes to the advancement of sustainable fabrication technologies, aiming to rival the adaptability and elegance of natural material systems.

2 Results and Discussion

The development of BEAVER was driven by the following design goals, ensuring robust performance, material versatility, and research adaptability:

- **Broad Biomaterial Compatibility** – The system was designed to support a diverse library of natural biopolymers (e.g., pectin, chitosan, cellulose) and biocomposites, accommodating a range of viscosities and rheological properties. Based on prior measurements using the previous pneumatic printer, successful extrusion typically required forces around 600 N. This capability was demonstrated through the successful printing of multiple parts using chitosan-cellulose biotic mixtures.
- **Dual-Extrusion System** – The system enables multi-material deposition for combining different biomaterials or creating compositional gradients, with positional accuracy within ±0.05mm. This functionality was validated through successful prints utilizing both extruders.
- **Scalability & Modularity** – The system allows for flexible upgrades, customization, and adaptation to various experimental needs. This was demonstrated through the discussion of modular component swaps and future upgrade paths.
- **Ease of Cleaning & Maintenance** – The extruder and cartridge components were designed to be removable and easily accessible to prevent material buildup and reduce contamination risk. This was confirmed by user feedback during test printing and routine cleaning.

- **Open-Source Design** – All hardware files, firmware configurations, and build instructions were made publicly available to promote accessibility and collaboration.

We emphasize that BEAVER achieves extrusion force control and deposition stability far exceeding prior pneumatic systems. With a peak extrusion force of 2,975 N and a volumetric flow rate of 775 mm^3/s, the system is capable of reliably extruding viscous hydrogels, including cellulose-chitosan blends. The extrusion force was estimated by scaling previously measured force requirements from the earlier pneumatic system, adjusted to account for the updated dimensions of the feedstock cartridge and nozzle in the new design. The volumetric flow rate was calculated based on the cross-sectional area of the smallest nozzle and the linear displacement speed of the plunger during extrusion.

The final design of BEAVER comprises a novel extruder design implemented for each dual extruders, a motion system tailored to meet the specific requirements of the extruders, a control board seamlessly integrated with both the extruders and the motion system, printer firmware configured to support its unique features, and slicer profiles and post-processing scripts compatible with free and open-source slicer software. To ensure repeatability and accuracy, the system incorporates stepper motors with micro-stepping control, guided by precision linear rails. Lead screws and timing belts are selected to minimize backlash and enable consistent, high-fidelity motion across print runs.

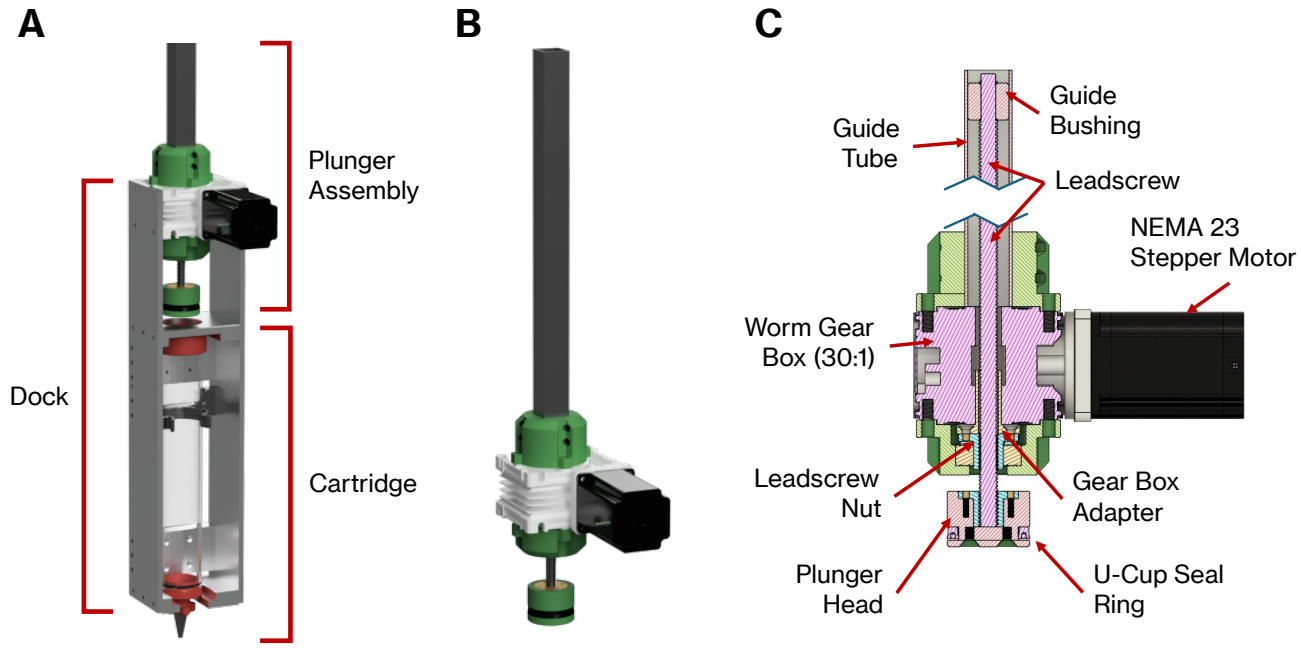

Figure 2: Extruder and plunger sub-assembly. A) Full rendered assembly of the extruder with the three main parts, the plunger assembly, the dock, and the cartridge. B) The plunger rendered subassembly which is responsible for creating the extrusion force. C) A cross-sectional view of the plunger assembly showing a NEMA 23 stepper motor with a 30:1 worm gear box is used to drive a leadscrew via an adapter to a leadscrew nut. The leadscrew is used to drive a plunger head that utilizes a U-cup sealing ring to push biomaterial through a cartridge. In order to constrain the leadscrew rotationally about its axis, a square guide bushing is fixed to the opposite end of the leadscrew and constrained via a guide tube.

Compared to the original proof-of-concept biotic 3D printer, BEAVER significantly improves upon precision, repeatability, and user accessibility. While the earlier system relied on a single pneumatic extruder prone to variability in flow rate due to material viscosity changes,

BEAVER utilizes motor-driven extrusion with micro-stepping and feedback-controlled hardware to enable more consistent and controlled deposition. In addition, the dual-extruder setup supports multi-material printing, features that were not possible with the single-extruder architecture. These improvements move beyond the original proof-of-concept and position BEAVER as a robust tool for research and applied fabrication with biotic materials. The completed printer is shown in **Figure 1A**, with its main components outlined in **Figure 1B**. The following sections provide a detailed discussion of each component's final design.

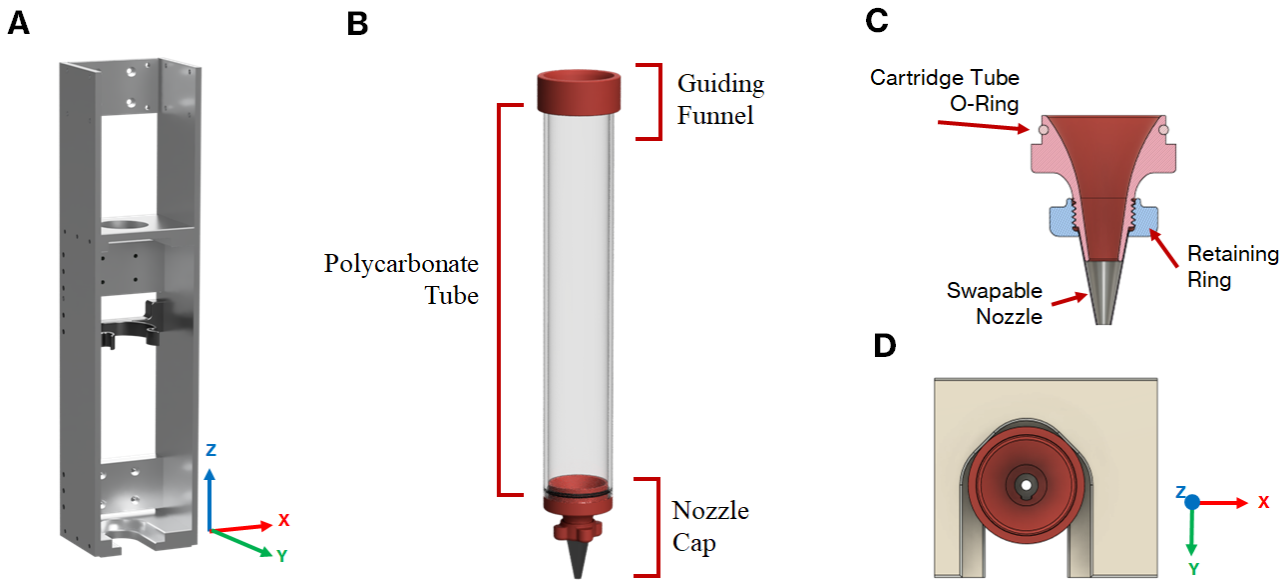

Figure 3: Extruder dock and cartridge subassemblies. A) The dock for the extruder which utilizes a top and bottom plate to locate the cartridge, and a compliant bracket to hold the cartridge. B) The final cartridge that holds the biomaterial feedstock. C) A cross-sectional view of the cartridge nozzle cap shows the gradual tapper going from the full diameter of the cartridge tube to the diameter of the swapable nozzle. D) Top-down view of the lower baseplate of the dock utilizes a V-groove to constrain the cartridge in the X and Y directions while the bottom of the baseplate constrains in the Z direction.

2.1 Extruder

The extruder was prioritized in the design process because it is the most critical component for 3D printing biomaterials. The final extruder design is a single-stage (**Figure 2A**), mechanical displacement-based system, similar to the commercial 3D PotterBot 10 XL, a single-extruder ceramic printer[22]. This choice was made to prioritize ease of cleaning, simplicity in maintenance, and improved longevity when compared to configurations such as a two-stage extruder which require secondary augers with more difficult to clean components. Functional requirements, including extrusion force (2,975 N), volumetric flow rate (775 mm^3/s), and other key parameters, were defined based on the performance of the previous biomaterial printer and the updated goals for the new extruder.

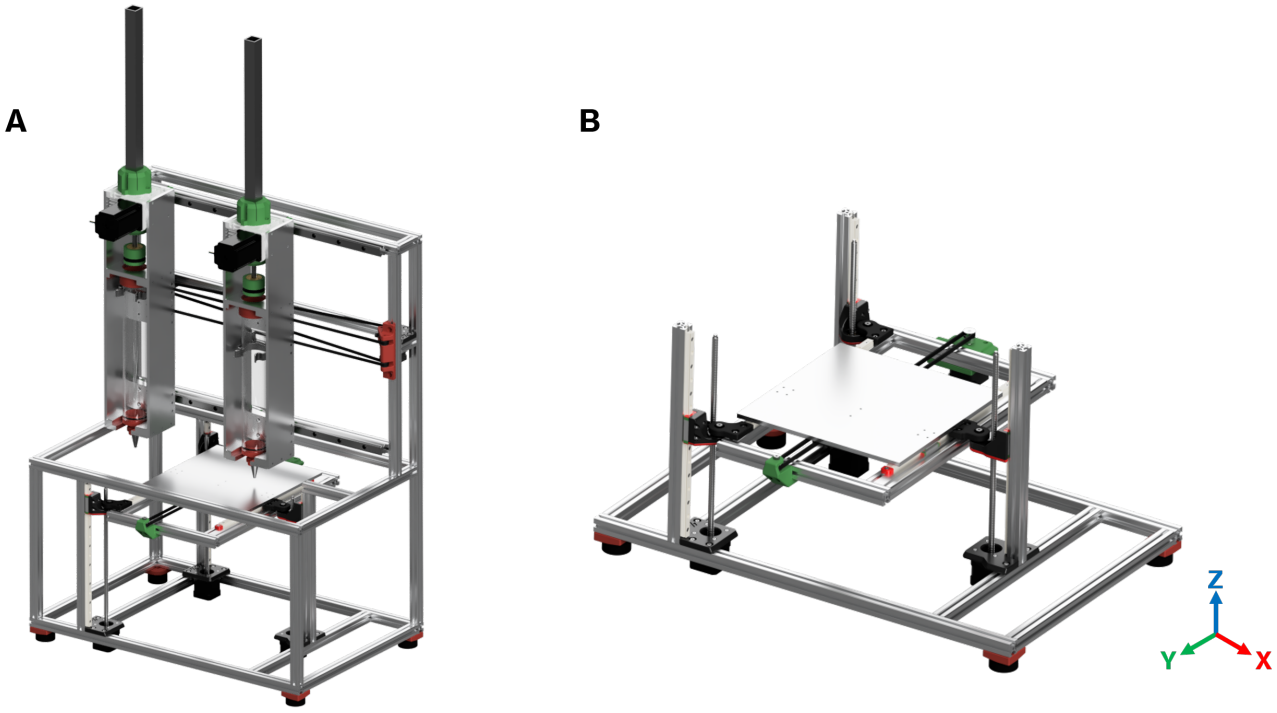

Figure 4: Renders of the BEAVER full assembly and build platform subassembly. A) A build platform is moved in the Y and Z directions while the dual extruders move in the X direction. Each extruder has its own drive stepper motor and timing belt, creating a redundant X axis called the A axis. B) Three linear rail and leadscrew pairs move the Y assembly in the Z direction. A stepper motor with a timing belt and linear rail pair move the build platform in the Z direction.

The overall envelope of one extruder is 183 mm × 110 mm × 930 mm. The final design of the extruder can be broken into three main parts, as outlined in **Figure 2A**. First, the plunger assembly, which is responsible for creating the extrusion force to deposit material, can be seen in **Figure 2B** and **Figure 2C**. The plunger assembly incorporates a 30:1 worm gearbox paired with a NEMA 23 stepper motor. The frame size of the extruder stepper motor was chosen to be NEMA 23 for its compatibility with the gearbox. The stack length of the stepper motor was selected to meet the torque requirement based on the extrusion forces required. This gear reduction ratio was optimized to balance the required extrusion force with sufficient speed for the desired volumetric flow rate. The gearbox's output shaft is connected to a leadscrew nut through a custom-designed hollow adapter, enabling the leadscrew to pass through the gearbox. This leadscrew configuration serves dual purposes: providing linear motion and functioning as the plunger rod for material extrusion. The diameter of the leadscrew was sized to withstand extrusion forces without buckling while remaining small enough to pass through the gearbox and adapter. To allow for linear motion, one end of the leadscrew is radially constrained using a square guide bushing and guide tube. At the opposite end, a plunger head was attached to the leadscrew. The plunger head features a U-cup sealing ring to maintain a proper seal during extrusion, ensuring consistent and reliable material flow.

The second main extruder component is the dock, which provides the structure of the extruder and acts as the loading-dock for the material cartridge (**Figure 3A**). A tool-free docking system facilitates rapid cartridge loading and unloading. For the high repeatability of loading cartridges into the dock, relevant degrees of freedom (DoF) were identified. Translation and rotation about the X and Y axes were identified as key DoF requiring constraint, while rotation about the Z

axis was negligible, and translation along the Z axis was insensitive due to nozzle offset compensation performed during probing. Inspired by principles of kinematic couplings, the dock constrains only the five critical DoF using a V-groove at each end of the cartridge. The V-grooves contact the cylindrical cartridge at two points on either end, constraining translation and rotation in the X and Y axes. The Z axis is supported by a planar lower baseplate, with an additional upper baseplate providing support during retraction. Although this configuration over-constrains the Z axis, the low sensitivity of this direction and minimal operational forces, along with the probing compensation, make it acceptable. For simplicity, the V-grooves and baseplates were integrated into a single component. During printing, the primary force acts along the Z axis. Downward plunger force engages the cartridge with the lower baseplate during extrusion, while retraction engages it with the upper baseplate, as shown in **Figure 3D**. Minor vertical movement between these baseplates is acceptable and aligns with typical 3D printer behavior, where nozzle lift prevents material dragging during travel. No significant forces act on the cartridge in the X and Y axes while docked, but a compliant retaining bracket was added for secure seating. This bracket is flexible enough for tool-free loading and unloading while ensuring consistent engagement with the V-grooves.

The final component of the extruder is the feedstock cartridge (**Figure 3B**), which was designed to match the material capacity of the previous biomaterial 3D printer and focused on simplicity and usability. To facilitate easy cleaning, the cartridge was designed to be fully disassembled without the need for tools or fasteners. A guiding funnel was incorporated at the top of the cartridge to ensure the extruder plunger head, particularly the U-cup sealing ring, could easily and reliably enter the cartridge. At the other end, a nozzle cap was designed to provide a gradual transition of the biomaterial from the full cartridge diameter to the outlet nozzle diameter which can be more clearly seen in **Figure 3C**. This cap also featured the ability to accommodate interchangeable nozzle tips, enabling the printer to achieve a broader range of printing resolutions. These nozzle tips could be swapped without the need of any tools. To accommodate for the potential height difference of the nozzle tips, a Z offset probe was implemented.

A dual-extrusion configuration, rather than a higher number of extruders, was selected to enhance material versatility while maintaining a manageable level of system complexity.

2.2 Motion System

The printer's build volume was set at 250 mm × 250 mm × 250 mm, selected to accommodate the typical dimensions of research prints while aligning with the build volumes of commonly used thermoplastic FFF printers for research and prototyping. For the motion system, a redundant axis was necessary for driving each of the independent dual extruders. The final design involved moving the build platform along the Y and Z axes while allowing the extruders to move independently along a redundant X-axis (**Figure 4A**). This configuration was chosen because it provided a simpler and more rigid structure, compared to moving the extruders along either of the other axes.

The Z axis used three MGN9 linear rails paired with Tr8x2 leadscrew integrated NEMA 17 stepper motors. The Y axis used two MGN9 linear rails and one NEMA 17 stepper motor with a GT2 timing belt. Each extruder is driven by its own NEMA 17 stepper motor and GT2 timing belt along a pair of HGR20 linear rails, enabling independent X-axis movement. In the printer's firmware, the second X axis is designated as the A axis. The MGR20 rails were mounted to the extruders at the greatest possible distance from each other to maximize radial stiffness and minimize deflection. It is worth noting that MGN12 leaner rails were found to be sufficient for the X axis, however, MGR20 linear rails were used because they were already owned.

The Z axis moves a platform that houses the Y axis and the build platform, shown in **Figure 4B**. To enable this motion, three leadscrew-and-rail pairs are used: two positioned at the left corners and one centered on the right side. This configuration avoids over-constraining the system, as three points are sufficient to define a plane. By connecting the platform to the leadscrew-rail pairs with 360-degree swivel bearings, the platform can move freely even if there are discrepancies in the relative positions of the three actuators. Any such discrepancies can be corrected during the printer's homing process, allowing the build platform to be leveled by adjusting the relative positions of the three actuators. The leadscrew-rail pairs were positioned along the “long” sides of the platform to maximize rigidity. This arrangement also allows the build platform to move in the Y direction beyond the bounds of Z leadscrew, helping to minimize the overall footprint of the printer. The design of the Z axis was inspired by the open-source Voron Trident FFF thermoplastic 3D printer project[23].

The Y axis employs a simple arrangement of a GT2 timing belt driven by a NEMA 17 stepper motor, with motion guided by two MGN9 linear rails. The use of two rails, positioned at either end of the build platform along the X direction, virtually eliminates moment forces caused by uneven weight distribution of material along the X axis during printing. While moment forces in the Y direction can still occur, it was determined that the two linear rail carriages can handle the maximum possible moment caused by an entirely lopsided 3D print. NEMA 17 motors were selected due to their widespread use in FFF printers, offering a well-established balance between torque and cost. They were deemed sufficient in force output, making larger motors unnecessary for this application.

2.3 Electrical Hardware and Software

The control system for the biomaterial 3D printer utilizes a Duet 3 Main Board 6HC paired with a Duet 3 Expansion Board 3HC, operating in Single Board Computer (SBC) mode with a Raspberry Pi 5. A Duet 3 Expansion Board 3HC was used in order to drive the extruder stepper motors, since the Duet 3 Main Board 6HC can only drive six stepper motors. This combination was chosen for its robust capabilities and compatibility with the printer’s requirements. The Duet 3 Main Board features integrated stepper motor drivers capable of driving high-current stepper motors, essential for the NEMA 23 extruder stepper motors, and sensor-less homing, which reduces the overall part count and design complexity. Its ability to connect over Wi-Fi allows for remote operation and monitoring, while its compatibility with a variety of sensors and add-ons ensures flexibility for future upgrades. Additionally, the Duet 3 is open-source, aligning with the goals of transparency and accessibility in the biomaterial printer’s design. Power for the system is provided by a 24V 42A power supply unit (PSU), which drives the control boards and stepper motors. The selected power supply was specified to accommodate the maximum possible current draw from all motors operating simultaneously, with an added safety margin, though such a scenario is unlikely during normal operation. The supply voltage was chosen to match the operating requirements of the stepper motors, ensuring reliable performance without overdesign. A separate 5V 5A PSU powers the Raspberry Pi 5, ensuring reliable operation of the SBC.

The Duet 3 runs on RepRapFirmware, which offers extensive customization options and conditional G-code scripting. A custom RepRapFirmware configuration profile was made for the biomaterial printer along with custom macro scripts to help enable the unique features of the printer. A key goal of the biomaterial 3D printer is user accessibility, even for non-experts. To achieve this, the workflow was designed to closely mimic that of traditional thermoplastic FFF printers. PrusaSlicer, an open-source commercial slicing software, was selected for generating G-code and tool paths for 3D models, with a custom printer profile tailored to the biomaterial printer. However,

no free or open-source slicer could fully support the redundant X-axis dual extruder design. To address this limitation, a post-processing script was developed to modify the G-code, enabling the printer's unique functionality.

2.4 Printing

Initial testing of the biomaterial printer focused on single extrusion prints (**Figure 5A** and **Figure 5B**) using the most viscous and challenging biomaterial recipe previously employed before moving on to simple and complex dual material prints (**Figure 5C-G)**. Achieving successful prints required iterative calibration to optimize print settings and refine the firmware configuration. After refinement, the printer successfully completed multiple single and dual extruder prints, producing high-quality and accurate results. Calibration prints, including standardized test cubes, were used to evaluate extrusion consistency and dimensional fidelity. Across multiple runs, dimensional error was consistently within ±0.3 mm in X, Y, and Z directions. We also monitored motor current and displacement per step to ensure consistent material flow, even with varying biomaterial viscosity. These validations confirm BEAVER's reliability as a scientific tool for biotic manufacturing.

Dual material tests were carried out using red- and blue-dyed versions of the same biomaterial used in single material prints. The dual material prints incorporated a multi-purpose purge wall during extruder swaps. A surrounding wall was printed around the part to prime the extruders before printing, doubling as an ooze shield to improve print quality. A purge wall was chosen over a priming tower to serve this dual purpose efficiently. Initial dual material prints employed a simple alternating layer design, where each layer alternated between the two extruders (**Figure 5C** and **Figure 5D**). This approach is the simplest form of dual material printing since both extruders do not print within the same layer. While this could theoretically be achieved on a single extruder printer by pausing the printer at each layer and manually swapping materials, the dual extruder system eliminates the need for manual intervention, significantly speeding up the process.

After successful alternating-layer prints, a more complex dual material geometry was tested. A bio-inspired hexagonal lattice with secondary material tubules was designed to mimic potential future research applications (**Figure 5E**). This design required precise alignment between the extruders, as any misalignment in X and Y coordinates would cause layer shifts. During these tests, a Z-lift was implemented during travel movements to prevent the active extruder nozzle from dragging through the layer deposited by the other extruder. This behavior underscores the value of the redundant-axis design, which enables independent movement of the dual extruders.

The test print still shows room for optimization, as the nozzle occasionally drags through layers, resulting in rough surface textures and material buildup on the nozzle (**Figure 5F** and **Figure 5G**). With further tuning of the print settings, these issues are expected to be resolved. Additionally, due to the time-dependent curing behavior of biotic materials, surface finish is influenced by both print parameters and post-processing conditions. Smoother finishes can be achieved through print tuning or mechanical post-processing such as sanding.

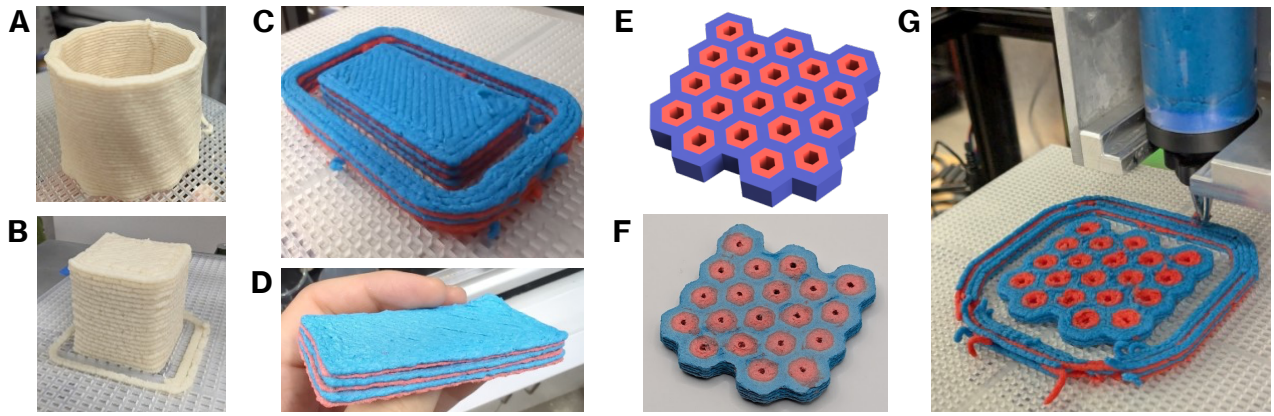

Figure 5: Examples of successful BEAVER single and dual material 3D prints. A) A single material test print of the biomaterial 3D printer of a vase-like structure. B) A calibration cube printed on the biomaterial 3D printer for testing and calibrating the dimensional accuracy and E-steps of the printer. An example of a simple dual material 3D printer in which the layers are printed with alternating extruders C) immediately after finishing printing and D) the same print fully dried. A wall can be seen printed around the model, this is both a priming tower and an ooze shield used when swapping between the extruders. E) A render of a dual material 3D print meant to replicate potential research uses for the printer in the future, a hexagonal lattice with inner tubules. F) The bio-inspired dual material print after fully drying and post-processing. G) The same bio-inspired model mid-print. The print can be seen with the same priming wall as in the previous dual material print.

3 Conclusions

The development of the biomaterial 3D printer, BEAVER, demonstrates a step toward a versatile and accessible platform for printing with biotic materials. By combining high-force stepper-driven extrusion with modular dual-material capabilities, it enables systematic exploration of biomaterial properties, compositional gradients, and sustainable fabrication – all in a fully open-source format. Its use of widely available components, supplemented by custom 3D-printed and machined parts, strikes a balance between accessibility and functionality. The printer has shown its capability to print biocomposites using both single and dual extruders. Single-material printing demonstrated that the system can handle viscous and challenging biomaterials, while dual-material printing highlighted its ability to carry out more complex extrusion workflows.

While the printer was primarily designed for biomaterials, its extruder design is versatile enough for other applications. It can process a wide range of viscous fluids, including ceramic greenware or even baking dough, demonstrating its adaptability. As an open-source platform, the design invites community-driven improvements and customization for specific applications, broadening its utility beyond biomaterials. Although the current system operates at ambient temperature, the control board supports thermal regulation, enabling future integration of heated cartridges, nozzles, or print bed for thermally sensitive materials. BEAVER serves as both a functional tool for printing biotic materials and a foundation for future innovations. Its ability to process challenging materials and support dual-material printing provides a foundation for continued exploration in bioprinting and biocomposite research.

Future developments for the biomaterial 3D printer include the integration of an AI-based autonomous print calibration system. Achieving this would require implementing new sensors on the printer. One proposed addition is a machine vision camera mounted beneath the extruder dock. The allocated clearance allows a Raspberry Pi camera to be positioned at the bottom of the dock without

interfering with the build platform or other components. This downward-facing camera would provide a 2D view of the print, a setup shown to optimize print settings for viscous fluid 3D printers[24]. Additionally, a secondary machine vision camera could be mounted on the printer frame, providing a 3D view of the build platform to monitor print quality and improve dimensional accuracy through further autonomous calibration[25]. Beyond computer vision, a strain gauge can be mounted on the plunger head, providing real-time extrusion force feedback. This hybrid system would combine displacement-based extrusion for material deposition with force feedback to predict and optimize print settings, facilitating the development of an expanding biomaterial library.

The printer also presents strong potential for integration into a fully autonomous lab, serving as a versatile platform for experimentation and innovation in additive manufacturing and AI for science[26–28]. Such an experimental platform would enable not only advanced biocomposite research but also investigations into topics like part geometry optimization, dual-material interactions, AI-generated 3D models, bio-inspired structures, and other cutting-edge fabrication and AI-driven strategies. By seamlessly integrating fabrication, testing, and iterative design within an AI-driven workflow, the autonomous lab would support a wide range of research objectives, extending beyond biocomposites to broader applications in advanced manufacturing and material science.

4 Materials and Methods

The following sections provide specific details regarding the materials, fabrication techniques, and engineering considerations used to construct the BEAVER system. It functions primarily as a design and replication guide with precision machining tips for those seeking to build or adapt the system. It includes information on component selection, manufacturing processes, and mechanical assembly best practices. In alignment with the open-source nature of the project, all CAD files, firmware, slicing scripts, and a complete bill of materials are publicly available at: https://github.com/lamm-mit/BEAVER.

4.1 Extruder Plunger

The extruder plunger was designed to use off-the-shelf or 3D-printed components whenever possible. However, certain components required more advanced fabrication methods due to the forces involved. The gear box adapter to leadscrew nut was fabricated using metal additive manufacturing in 316 stainless steel for durability and corrosion resistance.

The leadscrew and guide bushing also required more advanced manufacturing. A Tr8 leadscrew was purchased and modified on a manual lathe, with one end turned down to a smooth diameter and fitted with a groove for a retaining C-clip. Additionally, a keyway groove was added using a manual mill. The guide bushing was milled to the correct dimensions and had a through-hole bored using a drill and reamer, before finally using a broach to cut the keyway.

4.2 Extruder Dock

The walls of the dock and the upper linear rail adapter were cut from aluminum plate stock using a water jet. The compliant cartridge retaining bracket was 3D printed from polyethylene terephthalate glycol (PETG) for its flexibility, durability, and impact resistance, allowing it to deform under stress while maintaining structural integrity. All remaining components were fabricated using a milling machine.

The remaining parts had various main functions, such as constraining the cartridge, mounting the lower linear rail, and attaching to the X and A axis timing belts, but they all shared one critical dimension: the distance between the two dock walls. This meant that if one part was under the set tolerance, it would be too loose between the dock walls, and, inversely, if one part was over the tolerance, all remaining parts would be too loose.

To ensure precise relative tolerancing, these parts were milled simultaneously. Parts with identical footprints were temporarily bonded with cyanoacrylate glue to prevent shifting between operations. They were then clamped together in a milling vise in such a way as to maintain alignment while machining. This approach ensured all parts maintained consistent tolerances relative to each other. After the primary dimensions were milled, additional hole drilling and tapping operations were performed. For the cartridge locating components, a CNC mill was used to create the V-groove and holes/slots, allowing precise radii and off-axis features. These operations could also be completed with a manual mill and rotary table.

4.3 Motion System

To align with the open-source goal of the biomaterial printer, the motion system was designed to use accessible components. The frame is constructed from 2020 aluminum extrusion, and the stepper motors and timing belts are standard components used in most DIY and hobbyist printers. Custom parts for the motion system were designed to be manufacturable on consumer-level FFF 3D printers. The 2020 aluminum extrusions required their ends to be tapped and had clearance holes drilled in order to be assembled using blind joints. The build platform, which was water jet from aluminum plate stock, could also be purchased from online fabrication services.

4.4 3D Printed Parts

Final structural parts were printed in acrylonitrile styrene acrylate (ASA) due to its superior impact resistance, toughness, and durability compared to polylactic acid (PLA). Nonstructural parts were printed in polyethylene terephthalate glycol (PETG). ASA was chosen over acrylonitrile butadiene styrene (ABS) for its easier printability, reduced warping tendencies, better bed adhesion, and lower odor, while retaining similar mechanical properties. However, during the transition from PLA prototypes to the final ASA parts, bed adhesion and shrinkage still became challenges. To address these, PVA glue stick was applied to the build platform for better first layer adhesion, and some ASA parts were adjusted in Computer Aided Design (CAD) software or scaled in the slicer to account for shrinkage and minor warping. All parts were printed on a Bambu P1S printer with a 0.4 mm nozzle using Bambu Studio slicing software at a 0.20 mm layer height. Most parts utilized the "0.20mm Strength" default slicing profile, with minor adjustments made for specific parts to improve bed adhesion or dimensional accuracy.

4.5 Assembly

The assembly of the biomaterial printer required careful planning to ensure that all axes were square, and motion was smooth without binding. Precision machining best practices were followed, such as loosely assembling all bolted joints before sequentially bringing them to their final torque. Certain subassemblies, such as mounting the extruder plunder assembly to the linear rail and dock, required assembly in a specific order to avoid blocking access to fasteners during the process.

For the axis assembly, linear rails were initially loosely secured. Components attached to the linear rail carriages were fully assembled first. Starting at one end, the carriages were gradually moved along the rails while tightening each fastener to its final torque as the carriage passed it. This

ensured the linear rails were parallel, with the carriages maintaining consistent spacing during fastening.

The Z-axis assembly required a similar but more iterative process to ensure all three linear rails were parallel. In the first pass, all linear rails were loosened and retightened as the Y platform was progressively raised. In subsequent passes, two rails and then one rail were loosened and retightened. This stepwise process eliminated any strain in the linear rails, ensuring smooth motion and alignment.

4.6 Electrical and Software

All stepper motors and sensors were terminated using JST VH pin connectors to interface with the Duet 3 Main Board 6HC and Duet 3 Expansion Board 3HC. WAGO 222 connectors were used for the mains power leads, which were then routed to the 24V and 5V power supply units. All power lines were terminated with crimp-on spade and ring connectors for secure and reliable connections.

A custom RepRapFirmware configuration profile was developed for the biomaterial printer. The initial configuration was generated using the RepRap Config Tool but was extensively modified to accommodate the unique requirements of the custom dual extruders. Additionally, custom macro scripts were created to enhance workflow efficiency, including a material loading macro and an automatic nozzle offset macro for each extruder. Printer profiles tailored to the biomaterial printer were developed for PrusaSlicer. However, limitations in the slicer software necessitated a custom post-processing script. This script addresses the redundant X/A axis system driving the dual extruders by remapping G-code for the second extruder to the A axis and mirroring the movements of the first extruder to compensate for its opposing orientation. This ensures proper synchronization and functionality of the dual-extruder setup.

Materials List, Blueprints, Code Availability

The final materials list, blueprints, codes are available at: https://github.com/lamm-mit/BEAVER

Conflict of Interest

The authors declare no conflict of interest.

References

1. Geyer, R. Jambeck, J. Lavender Law, K. Production, use, and fate of all plastics ever made. *Sci. Adv*. **3**, e1700782 (2017). doi:10.1126/sciadv.1700782.
2. Stips, A., Macias, D., Coughlan, C., Garcia-Gorriz, E. & Liang, X. S. On the causal structure between CO2 and global temperature. *Sci. Rep.* **6**, 21691 (2016).

3. Law, B. E., Berner, L. T., Buotte, P. C., Mildrexler, D. J. & Ripple, W. J. Strategic Forest Reserves can protect biodiversity in the western United States and mitigate climate change. *Commun. Earth Environ.* **2**, 1–13 (2021).
4. Vijay, Y., Sanandiya, N. D., Dritsas, S. & Fernandez, J. G. Control of Process Settings for Large-Scale Additive Manufacturing With Sustainable Natural Composites. *J. Mech. Des.* **141**, (2019).
5. Gurunathan, T., Mohanty, S. & Nayak, S. K. A review of the recent developments in biocomposites based on natural fibres and their application perspectives. *Compos. Part Appl. Sci. Manuf.* **77**, 1–25 (2015).
6. John, M. J. & Thomas, S. Biofibres and biocomposites. *Carbohydr. Polym.* **71**, 343–364 (2008).
7. Gazdus, H. B., Shen, S. C., Lee, N. A. & Buehler, M. J. 3D Printable Biocomposites with Tunable Environmental Degradability. *3D Print. Addit. Manuf.* (2024) doi:10.1089/3dp.2024.0014.
8. Mohanty, A. K., Misra, M. & Hinrichsen, G. Biofibres, biodegradable polymers and biocomposites: An overview. *Macromol. Mater. Eng.* **276–277**, 1–24 (2000).
9. Mogas-Soldevila, L. & Oxman, N. Water-based Engineering & Fabrication: Large-Scale Additive Manufacturing of Biomaterials. *MRS Online Proc. Libr. OPL* **1800**, mrss15 (2015).
10. Ashby, M. F., Gibson, L. J., Wegst, U. & Olive, R. The mechanical properties of natural materials. I. Material property charts. *Proc. R. Soc. Lond. A.* **450:**123–140 (1995) doi:10.1098/rspa.1995.0075.
11. Fernandez, J. G. & Ingber, D. E. Manufacturing of Large-Scale Functional Objects Using Biodegradable Chitosan Bioplastic. *Macromol. Mater. Eng.* **299**, 932–938 (2014).
12. Abdul Khalil, H. P. S. *et al.* Bamboo fibre reinforced biocomposites: A review. *Mater. Des.* **42**, 353–368 (2012).
13. C. Shen, S. *et al.* Robust myco-composites: a biocomposite platform for versatile hybrid-living materials. *Mater. Horiz.* **11**, 1689–1703 (2024).
14. Billiet, T., Vandenhaute, M., Schelfhout, J., Van Vlierberghe, S. & Dubruel, P. A review of trends and limitations in hydrogel-rapid prototyping for tissue engineering. *Biomaterials* **33**, 6020–6041 (2012).
15. Duro-Royo, J., Van Zak, J. J., Tai, Y. J., Ling, A. S. & Oxman, N. *Parametric Chemistry Reverse Engineering Biomaterial Composites for Additive Manufacturing of Bio-Cement Structures across Scales*. *Prof. Oxman via Elizabeth Soergel* (CRC Press, 2017).

16. Sanandiya, N. D., Vijay, Y., Dimopoulou, M., Dritsas, S. & Fernandez, J. G. Large-scale additive manufacturing with bioinspired cellulosic materials. *Sci. Rep.* **8**, 8642 (2018).

17. Damoiseaux, R. UCLA's Molecular Screening Shared Resource: Enhancing Small Molecule Discovery with Functional Genomics and New Technology. *Comb. Chem. High Throughput Screen.* **17**, 356–368.

18. Janzen, W. P. Screening Technologies for Small Molecule Discovery: The State of the Art. *Chem. Biol.* **21**, 1162–1170 (2014).

19. Liu, J. *et al.* Current advances and future perspectives of 3D printing natural-derived biopolymers. *Carbohydr. Polym.* **207**, 297–316 (2019).

20. Duro-Royo, J. *et al.* Designing a Tree: Fabrication Informed Digital Design and Fabrication of Hierarchical Structures. *Proc. IASS Annu. Symp.* **2018**, 1–7 (2018).

21. Lee, N. A. *et al.* Sequential Multimaterial Additive Manufacturing of Functionally Graded Biopolymer Composites. *3d Print. Addit. Manuf.* **7**, 205–215 (2020).

22. 3D PotterBot 10 XL | 3D Potter. (2025, January 14) https://3dpotter.com/product/3d-potterbot-10-xl/.

23. VORON Trident. (2025, January 14) https://vorondesign.com/voron_trident.

24. Deneault, J. R. *et al.* Toward autonomous additive manufacturing: Bayesian optimization on a 3D printer. *MRS Bull.* **46**, 566–575 (2021).

25. Ganitano, G. S., Wallace, S. G., Maruyama, B. & Peterson, G. L. A hybrid metaheuristic and computer vision approach to closed-loop calibration of fused deposition modeling 3D printers. *Prog. Addit. Manuf.* (2023) doi:10.1007/s40964-023-00480-1.

26. Lee, N. A., Shen, S. C. & Buehler, M. J. An automated biomateriomics platform for sustainable programmable materials discovery. *Matter* **5**, 3597–3613 (2022).

27. Luu, R. K. *et al.* Learning from Nature to Achieve Material Sustainability: Generative AI for Rigorous Bio-inspired Materials Design. *MIT Explor. Gener. AI* (2024) doi:10.21428/e4baedd9.33bd7449.

28. Luu, R. K. & Buehler, M. J. Materials Informatics Tools in the Context of Bio-Inspired Material Mechanics. *J. Appl. Mech.* **90**, (2023).